Journal of Alloys and Compounds, 211/212 (1994) 378–380
JALCOM 140

Internal friction study of transformation dynamics in $BaTiO_3$ ceramics

J.X. Zhang[a], W. Zheng[a], P.C.W. Fung[b] and K.F. Liang[a]
[a]*Department of Physics, Zhongshan University, Guangzhou 510275 (China)*
[b]*Department of Physics, The University of Hong Kong (Hong Kong)*

Abstract

The internal friction (IF) and relative change of modulus of a doped semiconducting polycrystalline $BaTiO_3$ sample were measured by an inverted torsion pendulum with forced oscillation as the sample was heated in vacuum from −150 °C to 100 °C. Two IF peaks, P_1 and P_2, and two modulus, minima C_{3v}/C_{2v} and C_{2v}/C_{4v}, were observed corresponding to two phase transformations. All the IF peaks exhibit the characteristics of the first-order phase transformations. Each peak temperature is independent of frequency and the peak height increases with an increasing value of $(\dot{T}/\omega)^n$. A coupling coefficient of the phase interface to the oscillating stress is found to be $\alpha(\omega)=\alpha'\omega^{-l}$. For the two peaks P_1 and P_2 in the doped $BaTiO_3$ specimen, the values of n and l have been determined to be $n_1=0.225$, $n_2=0.190$, $l_1=0.101$, $l_2=0.204$. Our study indicates that the IF arises from the motion of phase interfaces during the process of the first-order phase transformation. A dynamic interaction model is proposed to explain the special features of IF during the two phase transformations.

1. Introduction

Barium titanate ceramic with a perovskite structure is well known for its piezoelectric and its positive temperature coefficient (PTC) effect, and this ceramic has a wide range of applications in industry. There are three ferroelectric phases in $BaTiO_3$ below the Curie point [1]. In the present paper, we investigate the dynamics of internal friction (IF) of two ferroelectric phase transitions of the semiconductor $BaTiO_3$ below the Curie point.

An internal friction (Q^{-1}) peak associated with the first-order phase transition (FOPT) was observed in the low-frequency range in a number of FOPT systems, such as FeMn [2–4], TiNi [4–7], AuCd [8,9], CuZnAl [10,11] and VO_2 [12]. Various theories have been presented for interpreting the origin of IF in the process of FOPT [3,13–15]. At present, there is no satisfactory theory generally accepted to explain the recently observed non-linear relations between Q^{-1} and the temperature rate $\dot{T}$ as well as Q^{-1} and the angular frequency ω [4–7].

2. Experimental

The semiconducting ceramic sample with nominal composition $(PbBa)(NbTi)O_3$ had a rectangular shape measuring $0.8\times3.0\times25.0$ mm^3; it was annealed at 1350 °C for 15 min after fabrication. The internal friction Q^{-1} and relative modulus M values were recorded for five frequencies ($f_1=0.10, f_2=0.266, f_3=0.707, f_4=1.88, f_5=5.00$ Hz) as a function of temperature, which was increased from −150 °C to 100 °C with a rate of $\dot{T}=0.25$ °C min^{-1}. The whole process was repeated at the values of $\dot{T}$ (0.5, 1.0, 2.5 and 5.0 °C min^{-1}). The strain amplitude of each measurement was about 5×10^{-5}, and the accuracy of Q^{-1} was within 1%. The phase transformation processes were also confirmed by X-ray and DSC measurements.

3. Results

Figures 1 and 2 show the temperature dependence of internal friction Q^{-1} and modulus M at five frequencies for various heating rates $\dot{T}$. Two groups of internal friction peaks, which correspond to the minima of the modulus, can be observed. The first IF peak, P_1, with peak temperature around −118 °C, was caused by the transition from the trigonal ferroelectric to orthorhombic ferroelectric phase (C_{3v}/C_{2v}). The second IF peak, P_2, is around −46 °C and corresponds to the transition from the orthorhombic ferroelectric to tetragonal phase (C_{2v}/C_{4v}).

It is clear from Fig. 1 and Fig. 2 that Q^{-1} increases with increasing temperature rate $\dot{T}$ (and variation in ω), but the relation is not linear in each case.

SSDI 0925-8388(94)00140-8

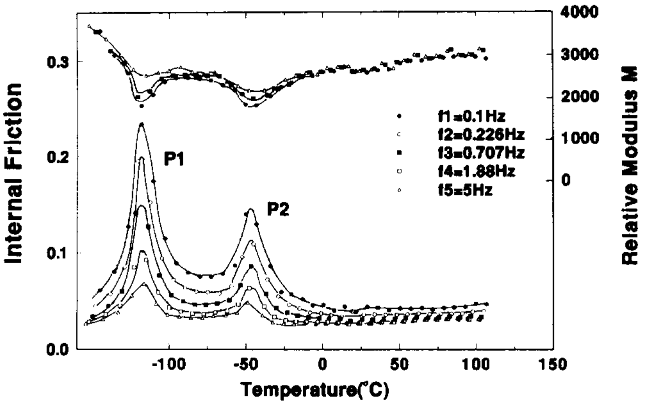

Fig. 1. Q^{-1} *vs.* T and M *vs.* T curves for different frequencies (0.1–5 Hz) at $\dot{T}=5$ °C min^{-1} in semiconducting BaTiO$_3$.

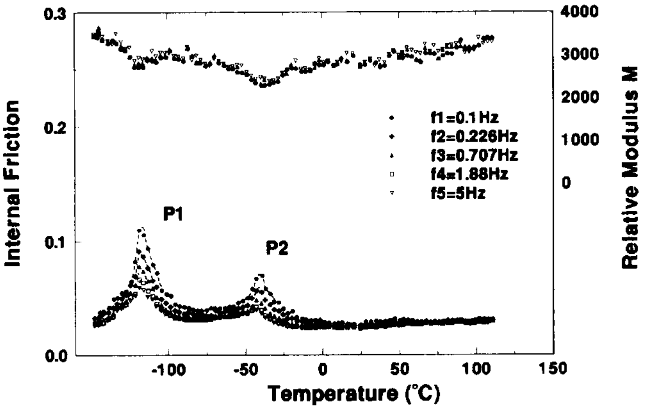

Fig. 2. Q^{-1} *vs.* T and M *vs.* T curves for different frequencies (0.1–5 Hz) at $\dot{T}=0.25$ °C min^{-1} in semiconducting BaTiO$_3$.

The IF experimental result for pure BaTiO$_3$ ceramics is similar to that for the doped ceramics, but the temperatures of the two peaks in pure BaTiO$_3$ are higher than those of the doped specimen.

4. Data analysis

Consider a unit area of phase interface (PI) moving along the x axis. The equation of motion of PI in the dynamical situation is [12, 16]

$$\rho\ddot{x}+\gamma\dot{x}+kx=\Delta G'+\Delta G_{\mathrm{a}}^{0}+\Delta G_{\mathrm{a}}^{\mathrm{dyn}}=f(t) \tag{1}$$

where ρ is the average mass density of PI, γ is the effective damping coefficient, and k is the dynamic restoring coefficient. $\Delta G'$ is an effective driving force of FOPT. $\Delta G_{\mathrm{a}}^{0}=\alpha(\omega)\sigma_{\mathrm{A}}\sin\omega t$ is the effective applied oscillating stress, ($\alpha(\omega)$ is a coupling factor). $\Delta G_{\mathrm{a}}^{\mathrm{dyn}}$ is an interaction driving force of FOPT and is equal to $C'\Delta G'\Delta G_{\mathrm{a}}^{0}$. Carrying out Laplace transformation on eqn. (1) and in view of the definition of IF, we have

$$Q^{-1}=\frac{\Delta\omega}{2\pi\omega}=N_{\mathrm{A}}\int_{0}^{P}\Delta G_{\mathrm{a}}^{0}\dot{X}\mathrm{d}t/(\pi\sigma_{\mathrm{A}}^{2}/\mu) \tag{2}$$

where N_{A} is the total area of the moving PI, and p is the period of oscillation. From [12], the IF during FOPT can be described as

$$Q^{-1}=A'(F)\alpha^{2}(\omega)(\dot{T}/\omega)^{n}+B'(F)\alpha^{2}(\omega)\omega \tag{3}$$

where F is the volume fraction of the product phase. The first term and second term in eqn. (3) for Q^{-1} are associated respectively with the moving PI arising from $\Delta G_{\mathrm{a}}^{\mathrm{dyn}}$ and the static PI arising from $\Delta G_{\mathrm{a}}^{0}$. From [12, 16], we also have an explicit representation of $\alpha(\omega)$:

$$\alpha(\omega)=\frac{2\epsilon_{0}Q^{-1}}{\Delta M/M}=\alpha'\omega^{-l}\qquad(0<l<1) \tag{4}$$

or

$$\frac{Q^{-1}}{\Delta M/M}=\frac{\alpha'\omega^{-l}}{2\epsilon_{0}} \tag{5}$$

leading to

$$\ln\left(\frac{Q^{-1}}{\Delta M/M}\right)=-l\ln\omega+\ln\left(\frac{\alpha'}{2\epsilon_{0}}\right) \tag{6}$$

where ϵ_0 is the phase transition strain and α' is a constant. Figure 3 shows the $\ln(Q^{-1}/(\Delta M/M))$ *vs.* $\ln\omega$ curves, from which the values of l are found to be 0.1 and 0.2 for P_1 and P_2. Consequently, eqn. (3) can be written with the values of l specified above, as

$$\frac{Q^{-1}}{\omega^{1-2l}}=A(F)\left(\frac{\dot{T}^{n}}{\omega^{n+1}}\right)+B(F) \tag{7}$$

where $A=A'(\alpha')^{2}$ and $B=B'(\alpha')^{2}$.

At the Q^{-1} peaks, the volume fractions of the new phase for various frequencies ω and T, $\dot{T}$ are practically the same because the shapes of the Q^{-1}–T curves are similar [16]. We can therefore use the peak values, i.e. Q^{-1} for different ω, T and $\dot{T}$, to plot Q^{-1}/ω^{1-2l} against $\dot{T}^{n}/(\omega^{n+1})$ (Fig. 4), taking n as the parameter for each

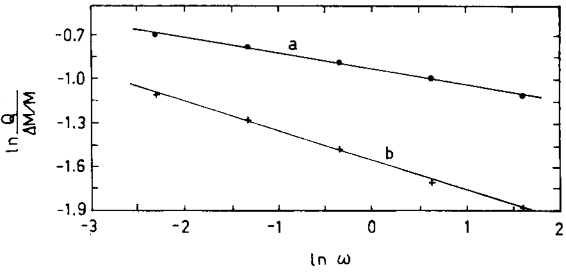

Fig. 3. ln ($Q^{-1}/\Delta M/M$) *vs.* ln ω plots for P_1 (a) and P_2 (b) of semiconducting BaTiO$_3$.

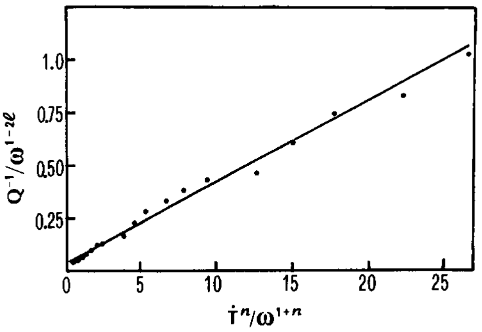

Fig. 4. Q^{-1}/ω^{1-2l} *vs.* $\dot{T}^n/\omega^{1-2l}$ *for* P_1 of semiconducting $BaTiO_3$ at IF peak.

TABLE 1. Values of the parameters of eqns. (3) and (6) inferred from the curves of Figs. 3 and 4

Peaks	$A(T_p)$	$B(T_p)$	l	n
P_1	0.047	0.030	0.100	0.250
P_2	0.017	0.019	0.204	0.225

graph. The value of n corresponding to the least-square fitting of the mentioned graph gives the desired n, while the slope is $A(F)$ and the intercept is $B(F)$. Corresponding to the peaks P_1 and P_2, the values of n are found to be $n_1 = 0.25$, $n_2 = 0.225$ (see Table 1). Equation (3) can now be expressed as the following for this particular sample:

$$Q^{-1} = \frac{A(T)\dot{T}^{0.25}}{\omega^{0.45}} + \frac{B(T)}{\omega^{0.8}} \quad \text{(for } P_1\text{)} \tag{8}$$

$$Q^{-1} = \frac{A(T)\dot{T}^{0.225}}{\omega^{0.63}} + \frac{B(T)}{\omega^{0.59}} \quad \text{(for } P_2\text{)} \tag{9}$$

The values for $A(T_p)$, $B(T_p)$ at the two peaks are listed in Table 1. From eqns. (8) and (9), Q^{-1} is a relatively stronger function of ω than $\dot{T}$.

5. Discussion

1. $A(T)$, $B(T)$ represent respectively the dynamic IF of the moving PI and the static IF of the static PI. From Table 1, both A and B have the same order of magnitude, and this result indicates that the IF caused by the static PI is also an important contribution to the total IF in the process of phase transition of $BaTiO_3$. Such a property is very different from those of other materials such as NiTi, FeMn and VO_2.

2. The exponent n is associated with the dynamic behaviour of the phase interface and determines the energy dissipation rate of the process of FOPT [12, 16], implying that n is an important parameter in FOPT dynamics. Up to now, we have investigated many FOPT systems with IF measurements, such as stress-induced and temperature-induced incommensurate/commensurate transition of NiTi(Fe) alloys, temperature-induced martensitic transformation of FeMn alloy and structural phase transformation in VO_2 ceramic. Similar results have been obtained for these studies. We are now in a position to formulate the FOPT with a phenomenological approach using both theoretical deduction and experimental data.

References

1 L. Carlsson, *Acta Crystallogr., 20* (1966) 459.
2 Y.N. Wang, Z.J. Yang, H. Zhu and J.C. Ma, *Acta Nanjing Univ., 7* (1963) 3.
3 Y.L. Ma and T.S. Ke, *Acta Phys. Sin., 20* (1964) 910.
4 J.X. Zhang and J.H. Li, *Acta Phys. Sin., 37* (1988) 363.
5 J.X. Zhang and L.Z. Luo, *Acta Phys. Sin., 37* (1988) 353.
6 Z.C. Lin, K.F. Liang, J.X. Zhang and W.G. Zeng, in *Proc. Int. Meeting on Advanced Materials, Tokyo, July 1988*, MRS, 1988.
7 K.F. Liang, Z.C. Lin and J.X. Zhang, in *Proc. of ICIFUAS-9, Beijing, China, July 1989*, International Academic Publishers, Beijing, 1990, p. 365.
8 Y.N. Wang, H.M. Shen, Z.R. Xu, Y.F. Zou, J.S. Zhu, Z.F. Zhang and Z.J. Yang, *J. Phys. (Paris), 42* (1981) C5-1049.
9 Z.J. Yang, Y.F. Zou, Z.F. Zhang and Y.N. Wang, *Acta Met. Sin., 18* (1982) 21.
10 J. Van Humbeck and L. Delacy, *J. Phys. (Paris), 44* (1983) C9-217.
11 M. Morin and G. Guenin, *J. Phys. (Paris), 44* (1983) C9-247.
12 J.X. Zhang and W.G. Zeng, *Proc. of ICIFUAS-9, Beijing, China, July 1989*, International Academic Publishers, Beijing, 1990, p. 313.
13 V.S. Postnikov, S.A. Gridnev, B.M. Dariskii and I.M. Sharshakov, *Nuovo Cimento, 33B* (1976) 324.
14 J.F. Delorme, R. Schmidt, M. Robin and P. Gobin, *J. Phys. (Paris), 32* (1971) C2-101.
15 W. Dejonghe, R. De Batist and L. Deleay, *Scr. Metall., 10* (1976) 1125.
16 J.X. Zhang, P.C.W. Fung and W.G. Zeng, *Phys. Rev. B.*, submitted for publication.